Materials Chemistry and Physics 236 (2019) 121792

Contents lists available at ScienceDirect

Materials Chemistry and Physics

journal homepage: www.elsevier.com/locate/matchemphys

SPEEK-based proton exchange membranes modified with MOF-encapsulated ionic liquid

Letícia G. da Trindade [a,d,*], Katiúscia M.N. Borba [a], Letícia Zanchet [a], Demétrius W. Lima [a], Aline B. Trench [b], Fernando Rey [c], Urbano Diaz [c], Elson Longo [b], Katia Bernardo-Gusmão [a], Emilse M.A. Martini [a,**]

[a] Laboratório de Reatividade e Catálise - Universidade Federal do Rio Grande do Sul, Av. Bento Gonçalves, 9500, P.O. Box 15003, Porto Alegre, 91501-970, Brazil
[b] Chemistry Dept. Federal University of São Carlos, C.P. 676, 13560-970, São Carlos, SP, Brazil
[c] Instituto de Tecnología Química, Universitat Politècnica de València-Consejo Superior de Investigaciones Científicas, Avenida de los Naranjos s/n, E-46022, Valencia, Spain
[d] Department of Chemistry, Universidade Estadual Paulista – Unesp, P.O. Box 473, 17033-360, Bauru, São Paulo, Brazil

HIGHLIGHTS

- Three ionic liquids were encapsulated in UiO-66 (Zr-MOF).
- Zr-MOF with encapsulated IL was incorporated into SPEEK membrane.
- SMOF/TEA2.5 membrane has shown the highest conductivity among SPEEK/MOF-IL membranes.

GRAPHICAL ABSTRACT

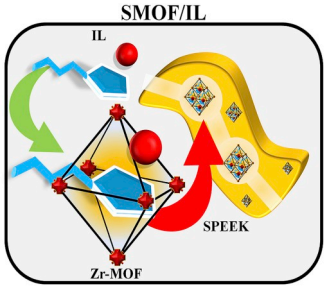

Sample	Proton Conductivity (mS cm^{-1}) 80 °C (60% RH)
SMOF/BH2.5	109
SMOF/BH5	54
SMOF/BM2.5	83
SMOF/BM5	43
SMOF/TEA2.5	140
SMOF/TEA5	65

ARTICLE INFO

Keywords:
Metal-organic framework
Ionic liquid
Sulfonated poly (ether ether ketone)
Zr-MOF/Ionic liquid-loaded proton exchange membrane

ABSTRACT

Ionic liquids (ILs) 1-butyl-3-methylimidazolium hydrogensulfate (BMI.HSO_4), 1-butylimidazole hydrogensulfate (BImH.HSO_4) and 3-triethylammonium propane sulfonic hydrogensulfate (TEA-PS.HSO_4) were encapsulated in UiO-66 (Zr-MOF) framework. These samples were incorporated into sulfonated poly (ether ether ketone) (SPEEK) polymer in different concentrations of IL. The influence of ionic liquid concentration encapsulated in Zr-MOF was evaluated through the morphology and thermal and chemical stability of the modified membranes. The incorporation of 7.5 wt% Zr-MOF in SPEEK produced membranes with high proton conductivity, making this the best mass ratio for the incorporation of the ionic liquids. Contact angle and swelling analysis indicate that the presence of these ionic liquids provides stability to the membrane, preventing it from absorbing high amounts of water. Mass ratios of 2.5 and 5.0 wt% of encapsulated ILs in Zr-MOF were also used. Proton conductivity results show that a higher concentration of ionic liquid generates agglomerates, limiting proton mobility in the membranes. Among the three ionic liquids tested, TEA-PS.HSO_4 presents the best proton conductivity values, between

* Corresponding author. Faculdade de Ciências, Unesp - Universidade Estadual Paulista "Júlio de Mesquita Filho", Av. Eng. Luiz Edmundo Carrijo Coube, 14-01 - Vargem Limpa, P.O. Box 473, 17033-360, Bauru, São Paulo, Brazil.
** Corresponding author. Laboratório de Reatividade e Catálise - Universidade Federal do Rio Grande do Sul, Av. Bento Gonçalves, 9500, P.O. Box 15003, Porto Alegre, 91501-970, Brazil.
E-mail addresses: lgt.gtrindade@gmail.com (L.G. da Trindade), emilse.martini@ufrgs.br (E.M.A. Martini).

https://doi.org/10.1016/j.matchemphys.2019.121792
Received 24 April 2019; Received in revised form 11 June 2019; Accepted 25 June 2019
Available online 26 June 2019

92 and 140 mS cm^{-1}. These results indicate that the Zr-MOF/TEA-PS.HSO_4 sample is a good candidate for use in proton exchange membrane for fuel cells.

1. Introduction

Clean energy generation with low or no CO_2 emissions has been abundantly researched and developed [1], with the promise of generating efficient and renewable energy to supply a sustainable future. Fuel cells (FCs) have stood out as a source of clean energy among numerous new technologies [2]. In this particular context, proton exchange membranes (PEMs) have been widely investigated in the last decades aiming to improve their performance in fuel cells [3]. In order for the membranes to have a better performance in FCs, they must be good proton conductors and electronically insulating at the same time. In addition, the materials used must provide thermal stability and prevent fuel crossover [4].

Nowadays, commercial membranes such as perfluorinated sulfonic acid (PFSA) membranes [5] are the most used in PEM fuel cells (PEMFCs) and, although they have significant proton conductivity, they present disadvantages such as high production cost, high fuel permeability, high dependence on water for good performance and operating only at temperatures below 80 °C [6]. In this context, alternative membranes have been developed seeking to obtain properties such as low cost, easy synthesis, good thermal and mechanical stability and eco-friendliness [7]. The poly(ether ether ketone) (PEEK), when it passes through the sulfonation process, obtaining SPEEK, has properties comparable to those of an ideal membrane. This process is made using concentrated sulfuric acid as sulfonating agent; $–SO_3H$ groups are introduced into the PEEK polymer chains to make them ion-exchangeable. Sulfonation aids in the transport of H^+ ions and increases the hydrophilicity of the polymer [8]. The high proton conductivity of SPEEK can be attributed to its high degree of sulfonation. However, the large amount of sulfonic groups attached to the polymer chain results in a lower chemical and thermal stability of this material.

Researches in search of alternatives to make SPEEK more stable for FC application have been carried out, among the alternatives studied; the use of ionic liquids stands out. Ionic liquids (ILs) are conductive salts which are liquid at temperatures below 100 °C and ambient pressure. ILs are composed of an organic cation and an organic or inorganic anion, and are studied and applied in various electrochemical devices [9]. Its properties are advantageous for application in membranes since they confer good chemical stability to the material and high ionic conductivity [10]. In a recent article, Zhao et al. [11] investigated the use of four different ionic liquids, [BMIm][BF_4], [BMIm]Cl, [DEMA][TfO] and [EIm][TfO], in membranes containing SPEEK and mesoporous silica, and obtained satisfactory proton conductivity results, around 15 mS cm^{-1} operating at 200 °C, when [BMIm][BF_4] ionic liquid was included in the SPEEK/SiO_2 membrane composition.

However, IL-doped SPEEK membranes undergo IL leaching during long-term operation, which results in loss of conductivity and leading to cell failure. In order to extend the service life of the membrane and to maintain the mechanical and thermal properties acquired with the use of ILs, inorganic materials such as clays and zeolites, as well as organic materials such as covalent organic (COFs) and metal-organic (MOFs) frameworks, are added to membranes with SPEEK/ILs [12].

Metal–organic frameworks (MOFs) are a new class of porous materials. Their structure is built typically from metal ions or connected through coordination bonds with organic ligands. MOFs are being investigated for countless applications and, among them; the most promising are storage and gas separation [13]. UiO-66 (UiO: University of Oslo), $Zr_6(\mu_3\text{-}O)_4(\mu_3\text{-}OH)_4(O_2C–C_6H_4–CO_2)_{12}$, is a highly crystalline zirconium-based MOF formed by octahedral $Zr_6O_4(OH)_4$, with 12-fold connections to the organic ligand 1,4-benzene-dicarboxylate (BDC). Its main advantages for use in FCs are related to its large surface area, stability and low electrical conductivity. Zhang et al. [14] prepared a hybrid material, SPEEK/HPW@MIL101, containing MOF MIL-101 (Cr), in the preparation of nanohybrid membranes for PEMFC applications, showing that this material is 7.25 times more conductive than a pristine SPEEK membrane. The effect of incorporating sulfonated MIL-101(Cr) on polymer membrane performance was studied by Li et al. [15]. At 75 °C/100% RH, the hybrid membranes achieved a proton conductivity of 0.306 S cm^{-1} with the incorporation of sul-MIL101(Cr), which is almost twice that of pure polymer membranes.

Here we present the encapsulation of 1-butylimidazole hydrogensulfate (BImH.HSO_4), 1-butyl-3-methylimidazolium hydrogensulfate (BMI.HSO_4) and 3-triethylammonium propane sulfonic hydrogensulfate (TEA-PS.HSO_4) ILs in Zr-MOF. The Zr-MOF/IL material is further inserted into the SPEEK membrane synthesis to fabricate proton exchange membranes by *casting* method. The particles and the modified membranes are investigated by structural and morphological characterization. The pristine SPEEK and the composite membranes are compared in terms of swelling, water uptake, oxidative stability and proton conductivity.

2. Experimental

2.1. Materials

The poly (ether ether ketone) (PEEK 450 PF) polymer was obtained from Victrex. The sulfuric acid (H_2SO_4 98%), methylene chloride (CH_2Cl_2), N,N-dimethylformamide (DMF, 99.8%), acetonitrile, ethyl acetate, N,N-dimethylacetamide (DMA, 99%), triethylamine (99%), 1-chlorobutane, 1-butylimidazol (98%), zirconium tetrachloride ($ZrCl_4$) and terephthalic acid were purchased from Aldrich and were used as received. The 1,3-propane sultone and ethyl acetate were obtained from Acros Organics and Vetec, respectively.

2.2. Ionic liquid synthesis

3-triethylammonium propane sulfonic hydrogensulfate (TEA-PS.HSO_4), 1-butylimidazole hydrogensulfate (BIm.HSO_4) and l-butyl-3-methylimidazolium hydrogensulfate (BMI.HSO_4) ILs were prepared following procedure found in the literature [16–18].

In order to synthesize the TEA-PS.HSO_4 IL, the 3-triethylammonium propane sulfonic acid (TEA-PS, 56.78 g) was dissolved in water (4.6 mL), and H_2SO_4 (14 mL) was added dropwise at 25 °C. The water was removed under vacuum at 90 °C yielding a colorless viscous liquid.

The BIm.HSO_4 IL was synthesized from the mixture of 1-butylimidazole (0.2 mol) with water (5 mL) and the H_2SO_4 (0.2 mol) was added dropwise. The reaction was carried out in an ice bath, with constant stirring at 25 °C. The product was dried under vacuum at 90 °C resulting in a brown liquid.

The BMI.HSO_4 IL is obtained from a cooled solution of l-butyl-3-methylimidazolium chloride (1 equivalent) in anhydrous CH_2Cl_2, in which H_2SO_4 (1 equivalent, 98%) is dripped dropwise. This solution was refluxed during 48 h at 25 °C; after this time, the mixture was evaporated with a rotary evaporator for complete removal of CH_2Cl_2, resulting in a colorless liquid [19].

2.3. Zr-MOF synthesis

The synthesis of the UiO-66 (Zr-MOF) framework was performed by combining the reactants, terephthalic acid and zirconium chloride (IV) ($ZrCl_4$), with 1:1 ratio. The synthesis was performed in DMF as described in the literature [20,21]. In an autoclave, 1.4 mmol of $ZrCl_4$, 1.4 mmol of

terephthalic acid and 3.6 mmol of DMF (0.09 mol L^{-1}), previously solubilized, were added. The reaction was kept in a greenhouse for 24 h at 125 °C. The obtained crystals were filtered under reduced pressure and dried in an oven during 4 h at 100 °C. The material was washed with methanol to remove the precursors from the synthesis and oven dried at 60 °C. After each washing, a XRD analysis was performed to monitor the increase in crystallinity of the material.

2.4. Ionic liquid encapsulation

The wet impregnation method was used for ionic liquid encapsulation in the Zr-MOF. This method consists of: (i) dissolving the ionic liquid in excess of ethanol; (ii) adding the Zr-MOF to this mixture and stirring during 4 h at 25 °C; and (iii) after obtaining a homogenous solution, oven-evacuating the solvent at 80 °C for 6 h, and the Zr-MOF/IL composite is obtained as a powder [22].

2.5. SPEEK preparation

The SPEEK membrane was obtained from the sulfonation of the PEEK polymer, as previously described in literature [23], with the aim of adding –HSO_3 groups, which allow the transport of H^+ ions. The PEEK polymer (10 g) was dissolved in H_2SO_4 (250 mL, 98%) under inert atmosphere; the solution was stirred for 20 h at 25 °C. Afterwards, the polymer solution was precipitated in excess of deionized water and ice under continuous stirring, and the polymer was washed to pH 5. The SPEEK polymer was dried under vacuum at 60 °C until its color turned yellow. The degree of sulfonation was determined by ^{1}H NMR spectrum, Fig. S1, according to the following equations [24]:

$$\frac{n}{12-2n} = \frac{\Delta H_E}{\Sigma AH_{A,A',B,B',C,D}} \qquad 0 \le n \le 1 \tag{1}$$

$$\text{Degree of sulfonation } (\%) = n \times 100 \tag{2}$$

where n is the sulfonation number, ΔH_E is the peak area of the neighbor hydrogen of SO_3H group signal and $\Sigma AH_{A,A',B,B',C,D}$ is the sum of the peak area of the signals corresponding to all the others aromatic hydrogens, named $H_{A,\ A',\ B,\ B',\ C,\ D}$. The ratio between the number of H_E (n) and the all the others aromatic hydrogens (12 - 2n) per repeat unit can be then obtained from the ratio between the peak area of H_E signal, (AH_E). In the present study the calculated degree of sulfonation was 66%.

2.6. Membranes preparation

Proportional amounts of SPEEK and Zr-MOF were mixed in DMA at 80 °C under constant stirring for 8 h. The homogeneous mixture was poured onto a petri dish and then dried in a vacuum oven during 24 h at 80 °C. The denominations of the prepared samples, along with their respective compositions, are shown in Table 1.

After evaluating the structure of the SPEEK/Zr-MOF membranes through ATR-FTIR and TG analysis and evaluating their proton conductivity in conditions of contoured relative humidity at 25 and 80 °C, the membrane with 7.5 wt% of Zr-MOF was chosen for addition of ionic liquid, because it had the highest proton conductivity among the samples studied.

The ionic liquids employed in the Zr-MOF were TEA-PS.HSO_4, BIm.HSO_4 and BMI.HSO_4. These composite membranes were prepared using 2.5 or 5 wt% of IL encapsulated in Zr-MOF. The chemical structure of SPEEK and the ionic liquids used are shown in Fig. 1, and the denominations given for the composite membranes and their respective compositions are shown in Table 2.

Table 1
Composition and sample designation of the composite membranes.

Sample	SPEEK (g)	Zr-MOF (wt.%)
S0	0.50	-
SMOF2.5	0.50	2.5
SMOF5	0.50	5.0
SMOF7.5	0.50	7.5
SMOF10	0.50	10.0

2.7. Characterizations

The Zr-MOF and Zr-MOF/IL powders were investigated using X-ray diffraction (XRD) and N_2 adsorption-desorption isotherm measurements. The XRD analyses were performed using a Rigaku detector with Cu Kα radiation (λ = 0.15406 nm) in the 2θ range of 2–80° using 0.05° min^{-1} steps. The Brunauer–Emmett–Teller (BET) method was using to determined the specific surface area at −196 °C with a partial pressure P/P0< 1. The pore size distribution was calculated using the N_2 adsorption-desorption isotherms and the classic theoretical model of Barrett, Joyner, and Halenda (BJH).

The attenuated total reflectance Fourier transform infrared spectroscopy (ATR-FTIR) spectra of SPEEK/Zr-MOF and SPEEK/Zr-MOF/IL membranes were measured with Bruker Alpha-P spectrometer in the range 4000–500 cm^{-1}. The thermal stability of the samples was determined by Thermal Gravimetric Analysis (TGA), using a TA Instruments Q-50 apparatus in the temperature range from 20 to 700 °C at 20 °C min^{-1} under N_2 atmosphere.

The crystal structures of the pure SPEEK and SPEEK/Zr-MOF-IL composite membranes were ascertained by X-ray diffraction (XRD) analysis, using a Rigaku X-ray diffractometer with a Cu-Kα radiation source, over the range $2^\circ \le 2\theta \le 80^\circ$.

The Zr-MOF and Zr-MOF/IL particles morphology and the cross-section of the synthetized membranes were observed using field-emission gun-scanning electron microscopy (FEG-SEM).

The topography images were analyzed by a Bruker Controur GT-K profilometer, with Vision 64 software. The contact angle measurement was performed using a Kruss DSA 30 at 25 °C, for to get information about the hydrophilicity of membranes surface.

The water uptake and the leaching measurements of the samples were determined by mass difference. The membranes were dried at 80 °C under vacuum for 24 h and immersed in deionized water at 80 °C for 24 h. The water uptake was obtained by the follow equation:

$$\text{Water uptake } (\%) = \frac{W_w - W_d}{W_d} \times 100\% \tag{3}$$

where W_w is the mass of the wet membrane and W_d is the mass of the dry membrane with absorbent paper.

The leaching out of Zr-MOF/IL composite was calculated using the formula:

$$\text{Leaching } (\%) = \frac{W_f - W_i}{W_f} \times 100\% \tag{4}$$

where W_i is initial mass of dry sample and W_f is the mass after immersion in deionized water and, dried in a vacuum oven at 80 °C for 24 h.

The oxidative stability of the samples was investigated by soaking 1.0 × 2.0 cm membrane pieces in Fenton's reagent (4 ppm Fe^{+2} in 3% H_2O_2) at 80 °C. For this test, the membranes were weighted (W_1), then placed in 20 mL of Fenton solution and kept at 80 °C for 24 h. Subsequently, the sample was collected by filtering, cleaned with deionized water, dried in a vacuum oven at 80 °C for 24 h, and then weighed (W_2). The oxidative stability can be seen as the complement of the weight loss, which was calculated using the formula bellow:

$$\text{Weight loss } (\%) = \frac{W_1 - W_2}{W_1} \times 100\% \tag{5}$$

Ion-exchange capacity (IEC) of all membranes was determined by titration [25]. Approximately 500 mg of the sample were immersed in 50 mL of 0.01 mol L^{-1} NaOH solution for 12 h at room temperature. The

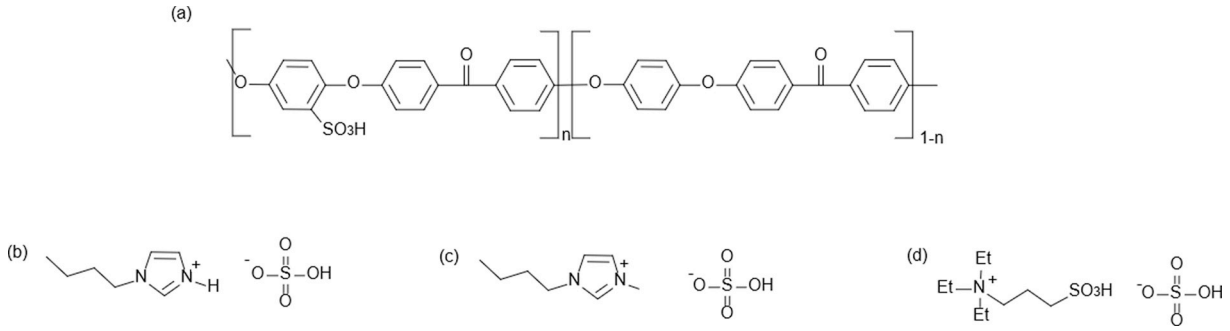

Fig. 1. Chemical structures of SPEEK (a), $BIm.HSO_4$ (b), $BMI.HSO_4$ (c) and TEA-PS.HSO_4 (d).

Table 2
Sample designation and composition of the membranes.

Sample	SPEEK (g)	Zr-MOF (wt. %)	Ionic liquid	Ionic liquid (wt. %)
S0	0.50	-	-	-
SMOF/TEA2.5	0.40	7.5	TEA-PS.HSO_4	2.5
SMOF/TEA5	0.40	7.5	TEA-PS.HSO_4	5.0
SMOF/BH2.5	0.40	7.5	BImH.HSO_4	2.5
SMOF/BH5	0.40	7.5	BImH.HSO_4	5.0
SMOF/BM2.5	0.40	7.5	$BMI.HSO_4$	2.5
SMOF/BM5	0.40	7.5	$BMI.HSO_4$	5.0

exchanged protons within the solutions (10 mL) were titrated with 0.01 mol L^{-1} HCl solutions. The IEC was calculated from the titration result by the following formula:

$$\text{IEC}\left(m_{equiv}\cdot g^{-1}\right) = \frac{(B-P)\times 0.01\times 5}{\text{weight drid membrane}} \quad (6)$$

where B is the volume of spent 0.01 mol L^{-1} HCl titrated to neutralize 10 mL of 0.01 mol L^{-1} NaOH, p is the volume of spent 0.01 mol L^{-1} HCl titrated to neutralize 10 mL of the aliquot after immersion of the membrane, and 5 is the conversion factor attributed to the dilutions.

The proton conductivity of the samples was determined by electrochemical impedance spectroscopy (EIS) method using an Autolab PGSTAT30 potentiostat from 10 Hz to 100 kHz, 0.01 V AC perturbation and open-circuit potential. The samples were cut into pieces of 20 mm × 15 mm, clamped by the edges between stainless steel electrodes and placed in a cell with controlled temperature and relative humidity (RH). The conductivity was measured at 25 and at 80 °C after the sample was equilibrated at 100 and 60% RH, respectively. The proton conductivity (σ) in the longitudinal direction was calculated by the following formula [26]:

$$\sigma = \frac{L}{R\,d\,W} \quad (7)$$

where L is the distance between the electrodes, d is the thickness and W the width of the membrane, and R is the resistance value calculated from EIS spectra.

3. Results and discussion

Fig. 2 (a) shows the ATR-FTIR spectra of S0, SMOF2.5, SMOF7.5 and SMOF10 samples. The pure SPEEK membrane (S0) has a strong absorption at 3440 cm^{-1} that can be related to the O–H from the SO_3H group. The peaks at 1491 and 1478 cm^{-1} are attributed to the aromatic C–C band. The peaks at 1224 and 1083 cm^{-1} are related to symmetric and asymmetric stretching vibrations of the SO_3H group in the SPEEK polymer [27]. For SMOF2.5, SMOF7.5 and SMOF10 similar spectra can be observed. These spectra have the same characteristic peaks of SPEEK, although it can be observed that the intensity of the peaks decreases with increasing amount of Zr-MOF in the membrane. The peaks at 1587 and 1394 cm^{-1} are attributed to the O–C–O asymmetric and symmetric stretching in the terephtalic acid ligand, and the peak at 554 cm^{-1} can be attributed to the Zr-(OC) asymmetric stretch [28,29]. These data confirm that Zr-MOF was successfully inserted into the polymer matrix.

The thermal properties of the pure and composite membranes were evaluated by TG analysis. The TG curves for pure SPEEK (S0) and modified SPEEK with 2.5, 7.5 and 10 wt% of Zr-MOF are shown in Fig. 2 (b). For the pristine SPEEK membrane (S0), we can observe three distinct steps of mass loss. The first, between 87 and 220 °C, is attributed to evaporation of water molecules absorbed in the sample; the second mass loss step, between 220 and 365 °C, is due to decomposition of

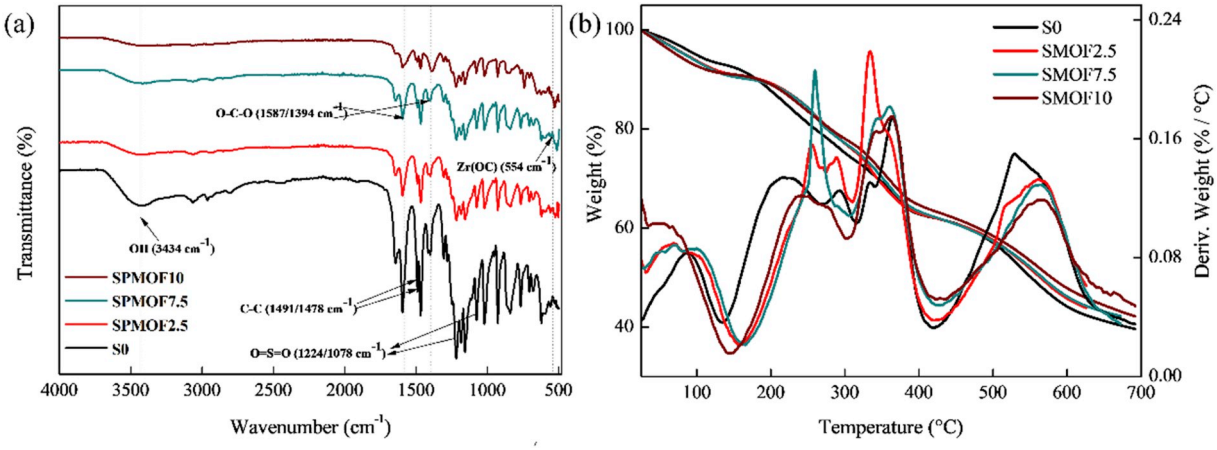

Fig. 2. ATR-FTIR spectra (a) and TG curves (b) for S0, SMOF2.5, SMOF7.5 and SMOF10 samples.

functional sulfonic acid groups; and the last step, at approximately 530 °C, may be attributed to the degradation of the main chain of the SPEEK membrane [30]. Membranes containing Zr-MOF exhibit the same behavior as pristine SPEEK polymer. Nonetheless, the second stage of mass loss starts at slightly higher temperature: approximately 260 °C for the samples with 2.5 and 7.5 wt% of Zr-MOF and 240 °C for the sample with 10 wt% of this material. Moreover, although the last degradation stage starts at the same temperature (approximately 560 °C), it is observed that, with the addition of Zr-MOF, the mass loss of the composite membranes decreased at the end of the stage. This result demonstrates that the incorporation of Zr-MOF to the polymer matrix confers thermal stability to the composite membrane. This additional thermal stability imparted to the polymer may be due to the hydrogen bonding interactions in the SPEEK/Zr-MOF membranes.

Table 3 shows the IEC and proton conductivity values obtained for SPEEK and modified SPEEK membranes with different Zr-MOF amounts. The IEC values increase with increasing amount of Zr-MOF added to the polymer, reaching a maximum of 2.04 mmol g^{-1} for the sample with 7.5 wt% Zr-MOF. This increase in the IEC value indicates that optimized ionic channels (clusters) are formed in the modified membranes via the mutual interactions between SPEEK and Zr-MOF, facilitating ion exchange. However, when the amount of Zr-MOF is increased to 10 wt%, the exchange capacity is reduced to 1.74 mmol g^{-1}. This behavior can be attributed to the fact that a high amount of Zr-MOF may block the membrane channels, hindering ion exchange.

The proton conductivity of pure Zr-MOF measured at 25 °C was 5.2 10^{-3} mS cm^{-1}. This value is 10^3 times smaller than that of the pure SPEEK measured in the same conditions. This large difference in the values indicates that the association of these two materials raises the conductivity of SPEEK because of the formation of clusters described above, which facilitates the ion exchange and thus increases conductivity. The data reveals that the incorporation of Zr-MOF in the polymer facilitates proton conduction when the material content is up to 7.5 wt %. On the other hand, when the Zr-MOF content is 10 wt%, the proton conductivity of the membrane is reduced. This reduction in protonic conductivity can be attributed to the fact that 10 wt% of Zr-MOF exceeds the maximum pore size of the polymer, thus making it difficult to diffuse and to occupy the water swelled pores in the polymer matrix [31]. For all membrane samples, proton conductivity increases with temperature and Zr-MOF content. The pristine membrane (S0) displays a proton conductivity of 77 mS cm^{-1} at 25 °C and 126 mS cm^{-1} at 80 °C. The SPEEK/MOF composite membranes show enhanced proton conductivity in both temperatures, reaching 141, 146, 172 and 129 mS cm^{-1} for SMOF2.5, SMOF5, SMOF7.5 and SMOF10, respectively, at 80 °C. From this increase in conductivity with addition of Zr-MOF we may infer that this material has unsaturated metal sites which can provide a significant amount of OH groups by hydrolysis. By hydrogen bonds, these OH groups can facilitate proton conduction by the Grotthuss mechanism [15,32]. The increase of the Zr-MOF amount in the polymer increased the number of metal sites, which facilitates the construction of the hydrogen bonding networks.

The results for SPEEK/MOF membranes with concentrations 2.5, 5, 7.5 and 10 wt% Zr-MOF show that an increase in Zr-MOF concentration causes an improvement in membrane conductivity, with a limit value reached when 7.5 wt% Zr-MOF in the polymer was used. The conductivity of the SMOF10 sample undergoes a drastic decrease in its value when compared to the SMOF7.5 membrane. Through thermal analysis it is evident that the increase in Zr-MOF concentration from 7.5 wt% to 10 wt% is also accompanied by loss of thermal stability in the material, since the SMOF10 sample decomposes at a lower temperature when compared to the other synthesized membranes. Considering these data, the quantity of Zr-MOF to be put on the SPEEK membrane was set at 7.5 wt%.

Table 3
Ion-exchange capacity (IEC) and proton conductivity (σ) and relative humidity (RH) of pure SPEEK (S0) and SPEEK/MOF samples with different Zr-MOF concentrations at 25 °C and 80 °C.

Sample	IEC (mmol g^{-1})	σ (mS cm^{-1})	
		25 °C (100% RH)	80 °C (60% RH)
S0	1.72	77	126
SMOF2.5	1.74	84	141
SMOF5	1.77	96	146
SMOF7.5	2.04	104	172
SMOF10	1.74	85	129

The Zr-MOF and Zr-MOF/IL materials were distinguished by XRD, BET and FEG-SEM analysis. The XRD analysis for Zr-MOF, Zr-MOF/BH5, Zr-MOF/BM5 and Zr-MOF/TEA5 samples are shown in Fig. 3.

The crystalline structure of the UiO-66 MOF can be confirmed by XRD analysis. The pure MOF diffractogram shows the crystallographic planes (111), (002), (113), (004), (115), (224), (046), and (137) relating to the 2θ peaks of 7.2°, 8.1°, 11.3°, 13.8°, 16.7°,21.9°,25.3°,30.6° and 32.8° [33]. It is possible to observe a large amorphous halo around 22° for the MOF/IL powders, presumably due to the presence of ionic liquid. Moreover, the characteristic peaks of the MOF associated to the planes (111), (002) and (113) are shifted to values less than 2θ, attesting to the increase in interplanar distances in relation to Zr-MOF without ionic liquid, which suggests that the IL is occupying the pores of the MOF structure. Furthermore, it is evident that the increase in the molar mass of the IL causes a decrease in peak intensity around 7.2°. This behavior suggests that a higher molar mass of the ionic liquid may hinder the crystallization of Zr-MOF.

The N_2 adsorption/desorption curves for pure Zr-MOF, Zr-MOF/BH5, Zr-MOF/BM5 and Zr-MOF/TEA5 are shown in Fig. 4.

It can be observed in the diagram that the volume of adsorbed gas is much higher for pure Zr-MOF; this is due to the lack of IL in the pores of the material. The BET method was used to determine the specific area; the following values were obtained: 987 m^2/g (Zr-MOF), 72 m^2/g (MOF/BM5), 49 m^2/g (MOF/BH5) and 42 m^2/g (MOF/TEA5). The pore volume was calculated by the BJH method; the following values were obtained: 0.52 cm^3/g (Zr-MOF), 0.074 cm^3/g (MOF/BM5), 0.063 cm^3/g (MOF/BH5) and 0.056 cm^3/g (MOF/TEA5). The decrease in specific area and pore volume values confirm that the ionic liquid fills the pores of the material. The MOF/TEA system presents the smallest specific area and the smaller volume of N_2 gas adsorbed in the Zr-MOF cavities, which confirms the results obtained by the XRD analysis and shows that the molar mass of ionic liquid is correlated with variation of the pores size.

The FEG-SEM images for pure Zr-MOF and MOF/IL particles are shown in Fig. 5.

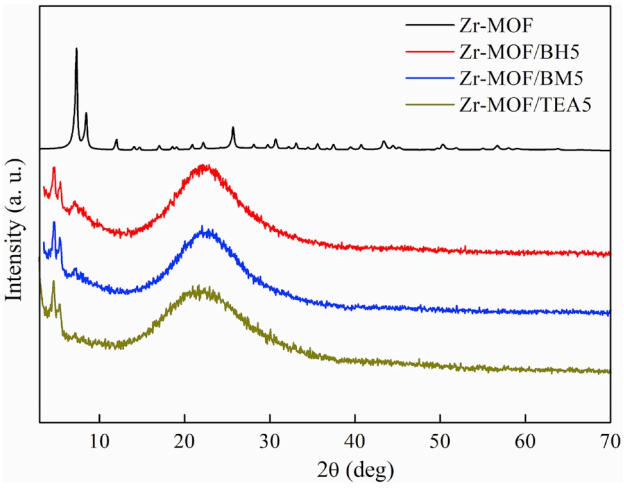

Fig. 3. XRD analysis of Zr-MOF, Zr-MOF/BH5, Zr-MOF/BM5 and Zr-MOF/TEA5.

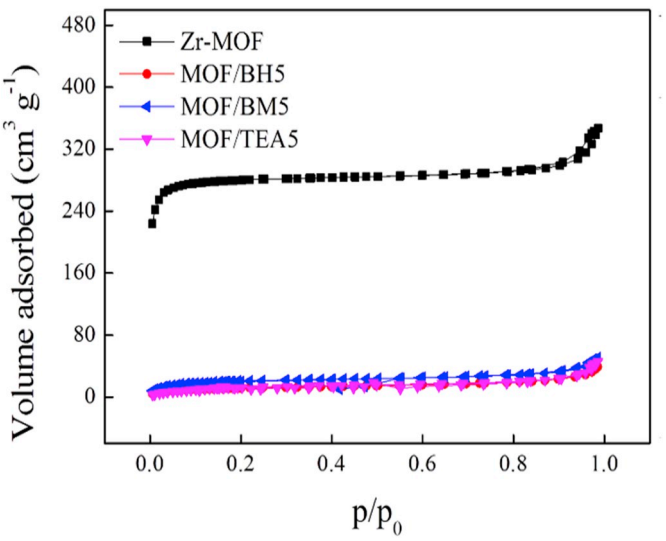

Fig. 4. N_2 sorption isotherms for Zr-MOF, MOF/BM5, MOF/BH5 and MOF/TEA5 samples.

It can be observed in Fig. 5 that the addition of ionic liquid in the Zr-MOF causes a decrease in the degree of agglomeration of the particles, and the presence of cubic structures is observed as the concentration of ionic liquid increases. This behavior can be attributed to an increase of the acidity of the medium with the addition of ILs. The pH values for the ionic liquids are 2.2, 3.8 and 1.3 for BIm.HSO_4, BMI.HSO_4 and TEAPS.HSO_4, respectively. As the acidity of the medium acidity increases, more cube-shaped crystals are observed, Fig. 5 (c, g and l), however these cubes present in varying sizes and gradually become larger with increasing IL concentration, as it can be seen in Fig. 5 (f, j and o). This behavior indicates that the ionic liquid is acting as a structure modulator, and the more acid the IL, more cubic structures are observed. However, when the amount of IL added is 2.5 wt%, the mean particle size does not change notably. When the amount of IL is doubled (5 wt%) an increase in particle size may be observed, nonetheless the mean particle size is practically identical for the three ILs.

After the characterization of Zr-MOF/IL particles, SPEEK modified membranes were manufactured with this material by the *casting* method. These composite membranes were morphologically and structurally characterized and compared to the SMOF7.5 membrane in order to evaluate the effects of the ionic liquids encapsulated in the Zr-MOF particles.

The ATR-FTIR spectra for SMOF/TEA2.5, SMOF/TEA5, SMOF/BH2.5, SMOF/BH5, SMOF/BM2.5 and SMOF/BM5 modified membranes are shown in Fig. 6.

In Fig. 6(a–c) it is shown that, regardless of the ionic liquid added, composite membranes retain the same characteristic peaks as pristine SPEEK and Zr-MOF. The peaks at 1245, 1075 and 1014 cm^{-1} are attributed to the –SO_3H group, referring to symmetrical and asymmetric O═S═O stretching vibrations [34]. The presence of the peak at 3440 cm^{-1} is another evidence of the presence of the –SO_3H group, since this is attributed to the O–H vibration of the sulfonic acid group [35]. The peak at 1648 cm^{-1} is attributed to the backbone C═O [35]. The evidence that Zr-MOF has been inserted into the membrane is the presence of the peaks at 1593 and 1395 cm^{-1} that are associated respectively with the asymmetric and symmetric oscillations of the O═C═O of the carboxylate group of terephthalic acid. In addition, the peak at approximately 555 cm^{-1} is attributed to the Zr-(OC) asymmetric stretch [36]. When the TEA-PS.HSO_4 IL is encapsulated in the Zr-MOF, the spectrum in Fig. 6(a) displays peaks at 2938 and 1496 cm^{-1} that are attributed to the axial deformation and the angular deformation of the C–H bond, respectively. The peaks at 1228, 1184 and 1035 cm^{-1} refers to asymmetric axial deformation of the S = O bond and axial deformation of the S–O bond of TEA-PS, respectively [37]. Moreover, the peaks at 1193 and 1151 cm^{-1} reports to antisymmetric SO_2 stretching and SOH bending modes, respectively [38]. When the BMI.HSO_4 was encapsulated, the peaks at 2964 and 2939 cm^{-1} in Fig. 6 (b) are assigned to C–H, CH_2 and CH_3 stretching peak on the lateral chain of the imidazole ring [39]. The peaks in 1574 and 1467 cm^{-1} refers to skeletal vibration peaks of imidazole ring, and the peaks at approximately 1195 and 1160 cm^{-1} are attributed to antisymmetric SO_2 stretching and SOH bending modes, respectively [38]. When the encapsulated ionic liquid is BImH.HSO_4 the peak at 1516 cm^{-1} in Fig. 6 (c) is attributed to in-plane stretching of the CH_2(N)CN ring. The peaks at 913 cm^{-1} and 818 cm^{-1} are assigned to N–H out-plane bending and NC(H)NCH bending vibrations, respectively [40]. Finally, the peaks at 1193 and 1156 cm^{-1} refers to antisymmetric SO_2 stretching and SOH bending modes, respectively [38].

The XRD patterns of the pure Zr-MOF, S0, SMOF7.5, SMOF/BH5, SMOF/BM5 and SMOF/TEA5 samples are shown in Fig. 7.

The influence of the ionic liquids in the formation of Zr-MOF inside the pores of the membrane is shown in the diffractograms of these composite membranes in Fig. 7. The diffraction pattern of Zr-MOF exhibit characteristic peaks of crystalline materials while the diffractogram of the SPEEK membrane (S0) presents a wide and flatted halo characteristic of a completely amorphous material [41]. The diffraction patterns of all composite membranes with Zr-MOF show the characteristic halo of the polymer membrane but also some flattened peaks that can be related to the formation of Zr-MOF in this membrane. It is interesting to observe the peak around 7.4° (2θ) in the diffraction patterns of composite membranes with the addition of ionic liquid. This peak is related to the overlap of MOF peaks (111) and (200), and can be considered a MOF crystallinity parameter in the membranes [42]. This peak is relatively intense in the composite membrane with BImH.HSO_4, but is attenuated in the membrane with BMI.HSO_4, and practically non-existent in the membrane with TEA-PS.HSO_4. This fact suggests a decrease in particle size, or in crystallinity, from the BImH.HSO_4 system (SMOF/BH5) to the BMI.HSO_4 system (SMOF/BM5). The Zr-MOF on the membrane with TEA-PS.HSO_4 (SMOF/TEA5) is practically amorphous. Probably, the molar mass or the size of the IL interferes with the formation of the Zr-MOF particle in the membrane pores. The BImH.HSO_4 ionic liquid molecule occupies little space inside the Zr-MOF pore and allows the development of more crystalline and probably larger Zr-MOF particles. The molecule of BMI.HSO_4 is larger than that BImH.HSO_4 and slightly disturbs the formation of these Zr-MOF nanoparticles. However, TEA-PS.HSO_4 is a very wide molecule, which occupies great of the membrane pore, and does not allow the full formation of the Zr-MOF nanoparticles, resulting in a poorly crystalline material.

TG analysis was performed to determine if the encapsulation of ILs into the Zr-MOF maintains the thermal stability of pristine Zr-MOF. The analysis of SMOF7.5, SMOF/TEA5, SMOF/BH5 and SMOF/BM5 membranes is shown in Fig. S2. It can be seen that the impregnation of Zr-MOF by TEA-PS.HSO_4, BIm.HSO_4 or BMI.HSO_4 ionic liquids maintains the thermal stability of SPEEK membrane with the addition of 7.5 wt% Zr-MOF. The SPEEK/MOF-IL composite membranes have the same behavior as the SPPEK/MOF membranes, that is, with the same three stages of degradation. The first step of mass loss is attributed to the waste of residual solvent or water. The second stage, which refers to degradation of the –SO_3H group in the range of 240–402 °C, shows more significant difference between the composite membranes. At this stage, the samples begin to degrade at a temperature approximately 20 °C lower than the membrane with 7.5 wt% Zr-MOF (SMOF7.5) and a larger mass loss of these membranes can be observed in this temperature range. This mass loss of the SPEEK/MOF-IL membranes may be associated to the loss of the HSO_4^- anion of the ionic liquid. The third stage starts at approximately the same temperature for all samples, and it assign to the SPEEK membrane main chair degradation.

Figure S3 shows that the average surface roughness of the SPEEK membrane surface is practically unchanged with the addition of 7.5 wt%

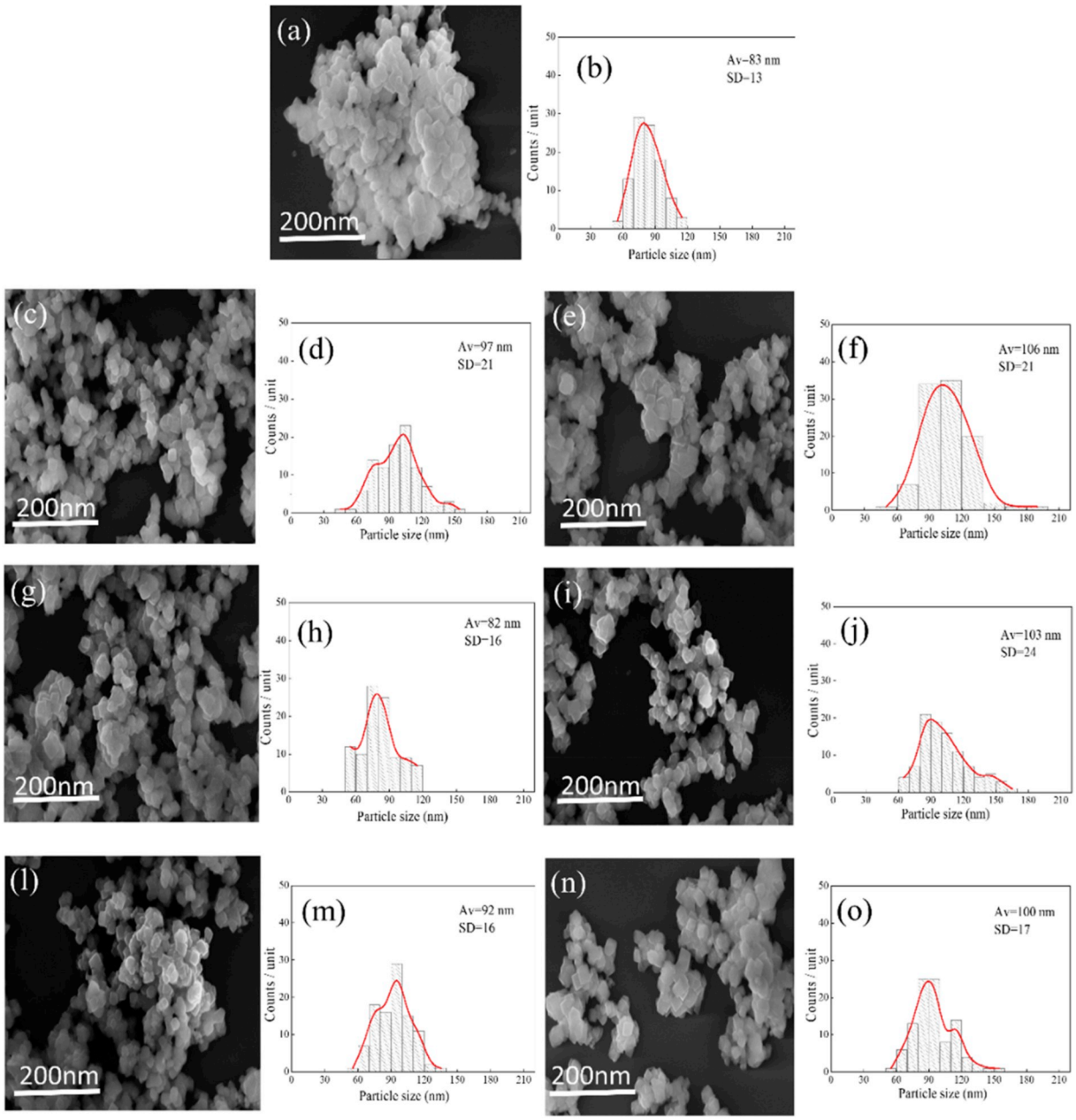

Fig. 5. FEG-SEM images and size distributions of Zr-MOF (a–b), MOF/BH2.5 (c–d), MOF/BH5 (e–f), MOF/BM2.5 (g–h), MOF/BM5 (i–j), MOF/TEA2.5 (l–m) and MOF/TEA5 (n–o) particles.

Zr-MOF, with a small decrease of 0.04 μm in the roughness value. For composite membranes SMOF/TEA5, SMOF/BH5 and SMOF/BM5, the roughness values were 1.05 μm, 0.77 μm and 0.75 μm, respectively. The SMOF/TEA5 composite membrane has a roughness of nearly 2.5 times greater than that of the SMOF7.5 sample, while SMOF/BH5 and SMOF/BM5 have a growth in roughness of approximately 1.8 times. This behavior may be associated with the cation size of the ionic liquids used. The size of the ionic liquid cations (0.86, 0.90 and 0.98 nm for $BImH^+$, BMI^+ and $TEA\text{-}PS^+$, respectively) indicates that only part of the cation is inserted into the Zr-MOF pore [43], because the Zr-MOF has a triangular opening of 0.6 nm, making it difficult for large molecules to enter [44]. As the $TEA\text{-}PS^+$ cation has greater volume, it may not have completely entered the pore, being mostly around it. Whereas the smaller $BImH^+$ and BMI^+ cations are able to accommodate better than $TEA\text{-}PS^+$ within the pores.

The cross-sectional images of pure SPEEK (S0) and SPEEK synthetized with the MOF/IL material are displayed in Fig. 8. It can be seen that the membranes were homogenously prepared, with no evident agglomerations in the SPEEK polymer matrix by MOF/IL particles.

In order to investigate whether the addition of the Zr-MOF/IL particles changes the wettability of the SPEEK membrane, the contact angle measurements were used to evaluate the surfaces of the membranes, Fig. 9 (a). In addition, in order to assess whether the change in the surface of the sample also influenced its water retention capacity, swelling tests were performed, and the results are shown in Fig. 9 (b).

It can be noted that, as the amount of IL increases from 2.5 to 5 wt%, the membranes surface become less hydrophilic and accordingly have a diminished water uptake ability. The contact angle increases from 85° to 93° and the water absorption is diminished from 70 to 67% for SMOF/BM2.5 and SMOF/BM5 composite membranes. For SMOF/BH2.5 and SMOF/BH5 samples, the values of contact angle were 82° and 100°, which led to a reduction in water retention from 76% to 62%. On the

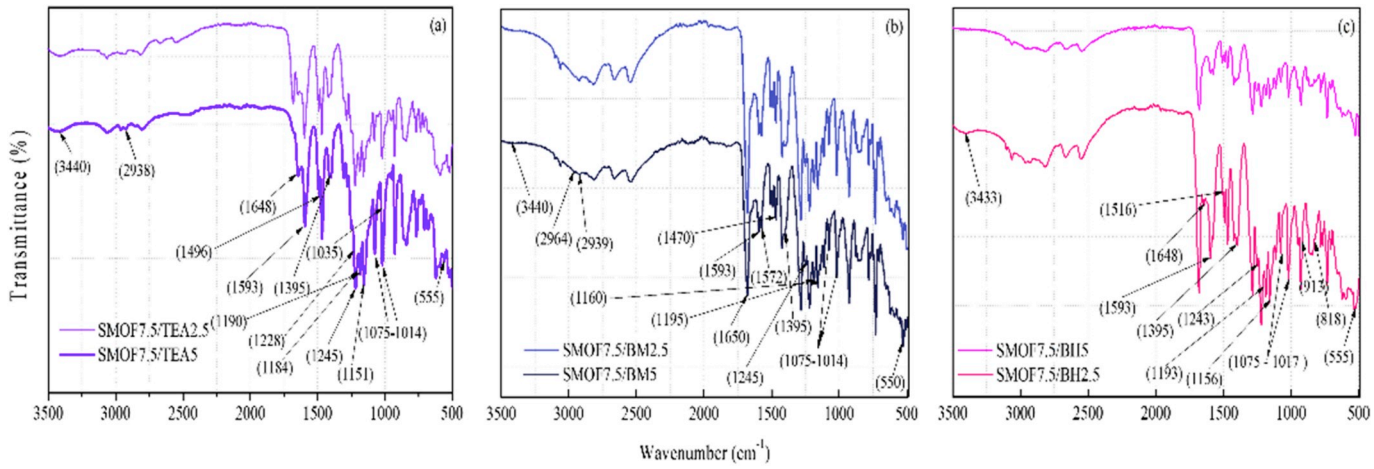

Fig. 6. ATR-FTIR spectra for SMOF/TEA2.5, SMOF/TEA5, SMOF/BH2.5, SMOF/BH5, SMOF/BM2.5 and SMOF/BM5.

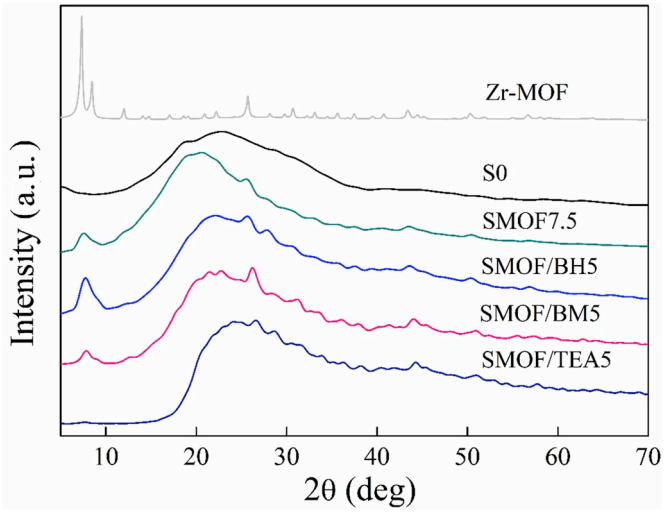

Fig. 7. XRD for Zr-MOF, S0, SMOF7.5, SMOF/BH5, SMOF/BM5 and SMOF/TEA5 samples.

other hand, for the composite membranes with TEA-PS.HSO_4 ionic liquid (SMOF/TEA2.5 and SMOF/TEA5) the contact angle had a low variance, from 78° to 81° and the water absorption was reduced from 94% to 78%, with increasing IL concentration. These data denote that the three ILs studied are in the pores of the Zr-MOF, improving the stability of the membrane and thus preventing its excessive swelling [45].

The SPEEK membrane with 7.5 wt% of Zr-MOF (SMOF7.5) exhibit a contact angle of 43°, indicating its high hydrophilicity, proven by its dissolution in water at 80 °C. The fact that this membrane has high water retention may be related to Zr-MOF structural elements, as pore size [46]. These factors facilitate the aggregation of water molecules within the pore, which are fixed by the formation of hydrogen bonds between the neighboring water molecules with the 1,4-benzoldicarboxylic acid binder [47].

Figure S4 shows the ability of the ionic liquid to exit the membrane in aqueous medium. The samples show the same leaching tendency, that is, with a growth in the quantity of IL encapsulated in the Zr-MOF, the leaching is increased. We can relate the pattern of leaching of the composite membranes with the interaction force of IL cations with the sulfonic group of SPEEK. The increase in leaching follows the order $BImH^+$ >BMI^+ >TEA-PS^+, indicating that the higher the cation, the greater the interaction of IL with Zr-MOF and SPEEK.

The weight loss test for oxidative stability, shown in Fig. 10, was performed to evaluate whether the pure Zr-MOF or the MOF/IL particles accelerate the chemical degradation of the SPEEK membrane. During PEMFC operation, reactive oxygen radicals (• OH, • OOH) can be generated by a chemical or electrochemical reaction between hydrogen and oxygen in the Pt catalyst [48].

The data reveal that the addition of 7.5 wt% Zr-MOF to SPEEK increases membrane degradation by 32%. However, when IL is encapsulated in the Zr-MOF particles, the tendency of chemical degradation of the polymer is reduced for all concentrations in comparation with SMOF7.5 sample. Nevertheless, it is observed that a rise in the amount of encapsulated IL also increases the tendency of membrane degradation. It is known that oxygen radicals react with weak terminal groups of the polymers [48]. In the case of SPEEK, the attack of the radical is possibly to the sulfonic group. Therefore, the addition of pure Zr-MOF accelerates the degradation of the membrane, because this material must be connected to these terminal groups by the formation of hydrogen bonds, further weakening it. This result can be confirmed by the contact angle and water retention measurements (Fig. 9): the addition of pure Zr-MOF increases the hydrophilicity tendency of the membrane and consequently its degree of swelling, making this composite membrane more fragile and consequently leading to its degradation. However, the encapsulation of IL in the Zr-MOF confers additional protection to these terminal groups, thus reducing decomposition. This decomposition process can be accelerated or slowed down depending on the amount of encapsulated ionic liquid, as shown in the results.

The IEC values for the SPEEK membranes modified with ionic liquid encapsulated in the Zr-MOF are shown in Table 4. The results show that the encapsulation of any of the three ionic liquids studied (BIm.HSO_4, BMI.HSO_4 and TEA-PS.HSO_4) decreases the IEC value compared to the membrane with 7.5 wt% Zr-MOF. It is also noted that an increase in the concentration of any of the ionic liquids reduces the IEC value. This reduction of the IEC values with the encapsulation of the ionic liquid in the Zr-MOF and with the increase of the amount of IL encapsulated can be attributed to the fact that these ionic liquids have large cations (0.86, 0.90 and 0.98 nm for $BImH^+$, BMI^+ and TEA-PS^+, respectively), which makes it difficult to insert them into the Zr-MOF pore (a triangular opening of side 0.6 nm). As they are not completely accommodated in the pore of the material, the ionic liquid cation may have an acid-base interaction with the –SO_3H groups causing decrease in the amount of free sulfonic acid groups available to release protons.

Conductivity measurements were performed in order to evaluate the effect that the encapsulation of the IL in the Zr-MOF particles has on the proton conductivity of the membranes. These measurements were performed under 2 conditions at 25 °C/100% RH and 80 °C/60% RH (Table 4).

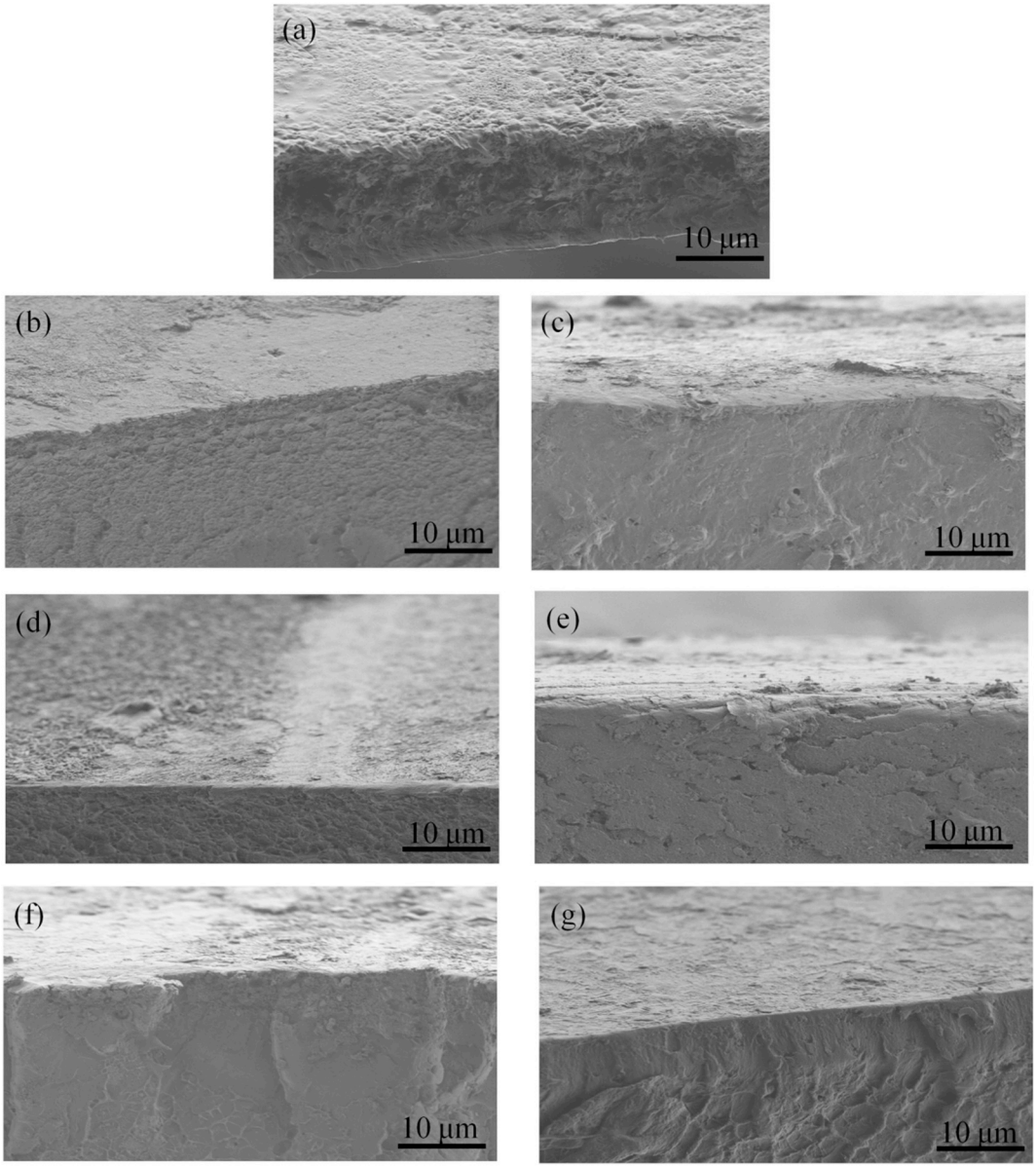

Fig. 8. Cross-sectional images of S0 (a), SMOF/BH2.5 (b), SMOF/BH5 (c), SMOF/BM2.5 (d), SMOF/BM5 (e), SMOF/TEA2.5 (f) and SMOF/TEA5 (g).

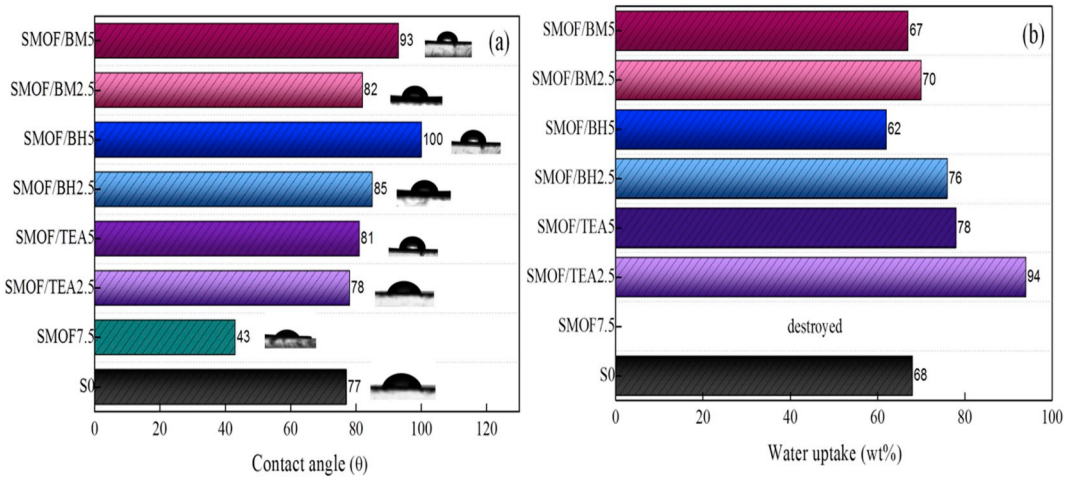

Fig. 9. Contact angle (a) and water uptake (b) for S0, SMOF7.5, SMOF/TEA2.5, SMOF7/TEA5, SMOF/BH2.5, SMOF/BH5, SMOF/BM2.5 and SMOF/BM5.

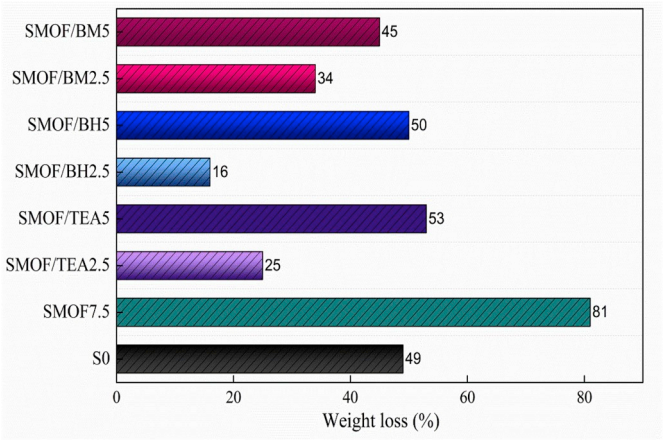

Fig. 10. Weight loss for oxidative stability assessment for S0, SMOF7.5, SMOF/TEA2.5, SMOF/TEA5, SMOF/BH2.5, SMOF/BH5, SMOF/BM2.5 and SMOF/BM5 samples.

Table 4
Ion-exchange capacity (IEC) and proton conductivity (σ) and relative humidity (RH) of SPEEK/MOF composite membranes with different amounts of ionic liquid at 25 °C and 80 °C.

Sample	IEC (mmol g^{-1})	σ (mS cm^{-1})	
		25 °C (100% RH)	80 °C (60% RH)
SMOF/BH2.5	1.76	88	109
SMOF/BH5	1.52	32	54
SMOF/BM2.5	1.69	64	83
SMOF/BM5	1.48	26	43
SMOF/TEA2.5	1.78	92	140
SMOF/TEA5	1.57	43	65

As listed in Table 4, the proton conductivity values of all composite membranes were smaller than that of the SMOF7.5 composite membrane (Table 3). This result can be related to the decrease in water uptake of the composite membrane when the ionic liquid was encapsulated in the Zr-MOF. The conductivity and the water uptake properties of the composite membranes follow the same order: SMOF7.5 > SMOF/TEA > SMOF/BH > SMOF/BM. The conductivity of the SMOF7.5 membrane is higher in both conditions studied, since the Zr-MOF can form hydrogen bonds between the neighboring water molecules with the 1,4-benzoldicarboxylic acid binder [47]. The values of activation energy (E_a) were obtained by the temperature dependence of conductivity using the Arrhenius model [49], as shown in Fig. S5. The results show that the E_a values exhibit a correlation with the amount of ionic liquid added in the membranes, increasing as these IL ratio increases in the samples. All membranes exhibit $E_a < 10\ kJ\ mol^{-1}$, suggesting a predominantly structural proton conduction mechanism (Grotthuss mechanism) [50]. However in this work, with the decrease in relative humidity in the system, appreciable values of conductivity were reached for the S0, SMOF7.5, SMOF/BH2.5 and SMOF/TEA2.5 membrane. Although the E_a values indicates the predominance of the Grotthuss mechanism, it is observed that with the decrease in relative humidity in the conductivity measurements there is evidence of ionic mobility, independently of the hydration conditions. Nevertheless, when the IL is encapsulated in the Zr-MOF pore, it prevents the water from entering, preventing the formation of hydrogen bonds decreased thus the proton conductivity. The data demonstrate that the ideal quantity of IL encapsulated for increasing the conductivity in both studied temperatures (25 and 80 °C) is 2.5 wt%, for the three ionic liquids used. The increase in the amount of encapsulated IL to 5 wt% significantly decreases all conductivity values. This reduction in proton conductivity may be related to the increase of particle agglomerations inside in the polymer channel, which can block the membrane channels preventing water retention [51]. The SMOF/-TEA2.5 composite membrane presented the highest conductivity values among membranes modified with MOF/IL particles. This behavior can be attributed to the fact that the TEA-PS.HSO_4 IL has a SO_3H group in the cation and a SO_4H group in the anion. These groups are protonic and their dissociation produce more H^+, thus contributing to the increase of proton conductivity. The proton conductivity measured at 80 °C is approximately 111% greater than the pure SPEEK membrane ($126\ mS\ cm^{-1}$) at the same temperature; this demonstrates that SMOF/TEA2.5 may be a promising membrane for use in PEMFC-type fuel cells.

4. Conclusions

SPEEK membranes modified with Zr-MOF and with IL encapsulated in Zr-MOF were produced by the *casting* method. SPEEK/MOF composite membranes with 7.5 wt% of Zr-MOF exhibit high conductivity, but dissolve in water at 80 °C. This behavior is attributed to structural factors of the MOF. The pore sizes of the MOF facilitate the aggregation of water molecules, which are fixed within the pores by hydrogen bonds. This increases conductivity, but also the degree of swelling, which causes the membrane dissolution when in prolonged contact with water. In order to increase thermal and chemical stability of the membrane, BImH.HSO_4, BMI.HSO_4 and TEA-PS.HSO_4 ILs were encapsulated at 2.5 wt% and 5 wt% by wet impregnation method. As consequence, higher contact angles and small water absorption are obtained. Among the three ILs studied in the SPEEK/Zr-MOF membranes, the composite membrane with 2.5 wt% of TEA-PS.HSO_4 encapsulated in the Zr-MOF (SMOF/TEA2.5 sample) showed higher water retention capacity and the best proton conductivity result between the studied SPEEK/MOF-IL composite membranes. This high conductivity is attributed to the fact that the TEA-PS.HSO_4 IL has a SO_3H group in the cation and a SO_4H group in the anion. These groups are protonic and their dissociation produces more H^+, thus contributing to the increase of proton conductivity. The results show that the SMOF/TEA2.5 membrane can be promising for PEMFC applications.

Acknowledgements

This study was financed in part by the Coordenação de Aperfeiçoamento de Pessoal de Nível Superior – Brasil (CAPES) – Finance Code 001. Moreover, this research was funded in part by Conselho Nacional de Desenvolvimento Científico e Tecnológico (CNPq) and Fundação de Amparo à Pesquisa do Estado de São Paulo (FAPESP) (2013/07296-2), which we are grateful for.

Appendix A. Supplementary data

Supplementary data to this article can be found online at https://doi.org/10.1016/j.matchemphys.2019.121792.

References

[1] H. Furukawa, O.M. Yaghi, Storage of hydrogen, methane, and carbon dioxide in highly porous covalent organic frameworks for clean energy applications, J. Am. Chem. Soc. 131 (2009) 8875–8883. https://doi.org/10.1021/ja9015765.
[2] A. Arshad, H.M. Ali, A. Habib, M.A. Bashir, M. Jabbal, Y. Yan, Energy and exergy analysis of fuel cells: a review, Therm. Sci. Eng. Process 9 (2019) 308–321. https://doi.org/10.1016/j.tsep.2018.12.008.
[3] T. Luo, S. Abdu, M. Wesslinga, Selectivity of ion exchange membranes: a review, J. Membr. Sci. 555 (2018) 429–454. https://doi.org/10.1016/j.memsci.2018.03.051.
[4] X. Cheng, J. Zhang, Y. Tang, C. Song, J. Shen, D. Song, J. Zhang, Hydrogen crossover in high-temperature PEM fuel cells, J. Power Sources 167 (2007) 25–31. https://doi.org/10.1016/j.jpowsour.2007.02.027.
[5] J. Jalili, S. Borsacchi, V. Tricoli, Proton conducting membranes in fully anhydrous conditions at elevated temperature: effect of Nitrilotris(methylenephosphonic acid) incorporation into Nafion- and poly(styrenesulfonic acid), J. Membr. Sci. 469 (2014) 162–173. https://doi.org/10.1016/j.memsci.2014.05.031.

[6] K.M. Mustafa, S.A.M. Alsaydeh, S.J. Zaidi, Chapter 12 - Beneficial Effect of Carbon Nanotubes on Membrane Properties for Fuel Cell Application, Advanced Nanomaterials for Membrane Synthesis and its Applications, Micro and Nano Technologies, 2019, pp. 271–293. https://doi.org/10.1016/B978-0-12-814503-6.00012-4.

[7] A.L. Khan, C. Klaysom, A. Gahlaut, X. Li, I.F.J. Vankelecom, SPEEK and functionalized mesoporous MCM-41 mixed matrix membranes for CO_2 separations, J. Mater. Chem. 22 (2012) 20057–20064. https://doi.org/10.1039/c2jm34885c.

[8] R.S.L. Yee, K. Zhang, B.P. Ladewig, The effects of sulfonated poly(ether ether ketone) ion exchange preparation conditions on membrane properties, Membranes 3 (2013) 182–195. https://10.3390/membranes3030182.

[9] H. Liu, H. Yu, Ionic liquids for electrochemical energy storage devices applications, J. Mater. Sci. Technol 35 (2019) 674–686. https://doi.org/10.1016/j.jmst.2018.10.007.

[10] R. Sood, C. Iojoiu, E. Espuche, F. Gouanvé, H. Mendil-Jakani, S. Lyonnard, Influence of different perfluorinated anion based Ionic liquids on the intrinsic properties of Nafion, J. Membr. Sci. 495 (2015) 445–456. https://doi.org/10.1016/j.memsci.2015.07.006.

[11] X. Wang, M. Jin, Y. Li, L. Zhao, The influence of various ionic liquids on the properties of SPEEK membrane doped with mesoporous silica, Electrochim. Acta 257 (2017) 290–300. https://doi.org/10.1016/j.electacta.2017.10.098.

[12] Q. Xin, T. Liu, Z. Li, S. Wang, Y. Li, Z. Li, J. Ouyang, Z. Jiang, H. Wu, Mixed matrix membranes composed of sulfonated poly(etheretherketone) and a sulfonated metal–organic framework for gas separation, J. Membr. Sci. 488 (2015) 67–78. https://doi.org/10.1016/j.memsci.2015.03.060.

[13] U. Mueller, M. Schubert, F. Teich, H. Puetter, K. Schierle-Arndta, J. Pastréa, Metal–organic frameworks—prospective industrial applications, J. Mater. Chem. 16 (2006) 626–636. https://doi.org/10.1039/B511962F.

[14] B. Zhangab, Y. Cao, Z. Li, H. Wu, Y. Yin, L. Cao, X. He, Z. Jiang, Proton exchange nanohybrid membranes with high phosphotungstic acid loading within metal-organic frameworks for PEMFC applications, Electrochim. Acta 240 (2017) 186–194. https://doi.org/10.1016/j.electacta.2017.04.087.

[15] Z. Li, G. He, Y. Zhao, Y. Cao, H. Wu, Y. Li, Z. Jiang, Enhanced proton conductivity of proton exchange membranes by incorporating sulfonated metal-organic frameworks, J. Membr. Sci. 262 (2014) 372–379. https://doi.org/10.1016/j.jpowsour.2014.03.123.

[16] F. Fiegenbaum, M.O. de Souza, M.R. Becker, E.M.A. Martini, R.F. de Souza, Electrocatalytic activities of cathode electrodes for water electrolysis using tetra-alkyl-ammonium-sulfonic acid ionic liquid as electrolyte, J. Power Sources 280 (2015) 12–17. https://doi.org/10.1016/j.jpowsour.2015.01.082.

[17] L. Zanchet, L.G. da Trindade, D.W. Lima, W. Bariviera, F. Trombetta, M.O. de Souza, E.M.A. Martini, Cation influence of new imidazolium-based ionic liquids on hydrogen production from water electrolysis, Ionics. https://doi.org/10.1007/s11581-018-2803-0, 2018.

[18] K. Niknam, M. Damya, 1-Butyl-3-methylimidazolium hydrogen sulfate [bmim]HSO4: an efficient reusable acidic ionic liquid for the synthesis of 1,8-dioxo-octahydroxanthenes, J. Chin. Chem. Soc. 56 (2009) 659–665. https://onlinelibrary.wiley.com/doi/epdf/10.1002/jccs.200900098.

[19] J. Fraga-Dubreuil, K. Bourahla, M. Rahmouni, J.P. Bazureau, J. Hamelin, Catalysed esterifications in room temperature ionic liquids with acidic counteranion as recyclable reaction media, Catal. Commun. 3 (2002) 185–190. https://doi.org/10.1016/S1566-7367(02)00087-0.

[20] A. Ghorbanpour, L.D. Huelsenbeck, D.-M. Smilgies, G. Giri, Oriented UiO-66 thin films through solution shearing, CrystEngComm 20 (2018) 294–300. https://doi.org/10.1039/C7CE01801K.

[21] N. Karimian, H. Fakhri, S. Amidi, A. Hajian, F. Arduini, H. Bagheri, A novel sensing layer based on metal-organic framework UiO-66 modified with TiO2-graphene oxide: application to rapid, sensitive and simultaneous determination of paraoxon and chlorpyrifos, New J. Chem. 00 (2018) 1–11. https://doi.org/10.1039/x0xx00000x.

[22] F.P. Kinik, A. Uzun, S. Keskin, Ionic liquid/metal–organic framework composites: from synthesis to applications, Chem. Sus. Chem. 10 (2017) 2842–2863. https://doi.org/10.1002/cssc.201700716.

[23] L.G. da Trindade, E.C. Pereira, New anhydrous polymer membranes of SPEEK/zeolite/ionic liquid for fuel cell application, Eur. J. Inorg. Chem. 2017 (2017) 2369–2376. https://doi.org/10.1002/ejic.201601559.

[24] L.G. da Trindade, L. Zanchet, J.C. Padilha, F. Celso, S.D. Mikhailenko, M.R. Becker, M.O. de Souza, R.F. de Souza, Influence of ionic liquids on the properties of sulfonated polymer membranes, Mater. Chem. Phys. 148 (2014) 648–654. https://doi.org/10.1016/j.matchemphys.2014.08.030.

[25] L.G. Trindade, M.R. Becker, F. Celso, C.L. Petzhold, E.M.A. Martini, R.F. Souza, Modification of sulfonated poly(ether ether ketone) membranes by impregnation with the ionic liquid 1-butyl-3-methylimidazolium tetrafluoroborate for proton exchange membrane fuel cell applications, Polym. Eng. Sci. 56 (2016) 1037–1044. https://doi.org/10.1002/pen.24334.

[26] L.G. da Trindade, L. Zanchet, K.M.N. Borba, J.C. Souza, E.R. Leite, E.M.A. Martini, Effect of the doping time of the 1-butyl-3-methylimidazolium ionic liquid cation on the Nafion membrane proprieties, Int. J. Energy Res. (2018) 1–9. https://doi.org/10.1002/er.4096.

[27] S. Park, H. Kim, Preparation of a sulfonated poly(ether ether ketone)-based composite membrane with phenyl isocyanate treated sulfonated graphene oxide for a vanadium redox flow battery, J. Electrochem. Soc. 163 (2016) A2293–A2298. https://doi.org/10.1149/2.0731610jes.

[28] J. Ding, Z. Yang, C. He, X. Tong, Y. Li, X. Niu, H. Zhang, UiO-66(Zr) coupled with Bi_2MoO_6 as photocatalyst for visible-light promoted dye degradation, J. Colloid Interface Sci. 497 (2017) 126–133. https://doi.org/10.1016/j.jcis.2017.02.060.

[29] Y. Luan, Y. Qi, Z. Jin, X. Peng, H. Gao, G. Wang, Synthesis of a flower-like Zr-based metal–organic framework and study of its catalytic performance in the Mannich reaction, RSC Adv. 5 (2015) 19273–19278. https://doi.org/10.1039/C4RA15257C.

[30] Z. Zhao, C. Pan, G. Jiang, M. Zhong, B. Fei, Electrochemical properties of SPEEK/Epoxy/Graphene Oxide composites as proton exchange membrane, Int. J. Electrochem. Sci. 13 (2018) 2945–2957. https://doi.org/10.20964/2018.03.03.

[31] J. Li, G. Xu, X. Luo, J. Xiong, Z. Liu, W. Cai, Effect of nano-size of functionalized silica on overall performance of swellingfilling modified Nafion membrane for direct methanol fuel cell application, Appl. Energy 213 (2018) 408–414. https://doi.org/10.1016/j.apenergy.2018.01.052.

[32] M.B. Bajestani, S.A. Mousavi, Effect of casting solvent on the characteristics of Nafion/TiO_2 nanocomposite membranes for microbial fuel cell application, Int. J. Hydrogen Energy 41 (2016) 476–482. https://doi.org/10.1016/j.ijhydene.2015.11.036.

[33] L. Valenzano, B. Civalleri, S. Chavan, S. Bordiga, M.H. Nilsen, S. Jakobsen, K. P. Lillerud, C. Lamberti, Disclosing the complex structure of UiO-66 metal organic framework: a synergic combination of experiment and theory, Chem. Mater. 23 (2011) 1700–1718. https://doi.org/10.1021/cm1022882.

[34] K. Charradia, Z. Ahmeda, P. Arandac, R. Chtourou, Silica/montmorillonite nanoarchitectures and layered double hydroxide-SPEEK based composite membranes for fuel cells applications, Appl. Clay Sci. 174 (2019) 77–85. https://doi.org/10.1016/j.clay.2019.03.027.

[35] A.G. Al Lafi, The sulfonation of poly(ether ether ketone) as investigated by two-dimensional FTIR correlation spectroscopy, J. Appl. Polym. Sci. 132 (2015) 41242. https://doi.org/10.1002/app.41242.

[36] Y. Han, M. Liu, K. Li, Y. Zuo, Y. Wei, S. Xu, G. Zhang, C. Song, Z. Zhang, X. Guo, Facile synthesis of morphology and size-controlled zirconium metal–organic framework UiO-66: the role of hydrofluoric acid in crystallization, CrystEngComm (2015) 6434–6440. https://doi.org/10.1039/C5CE00729A.

[37] S. Liu, C. Xie, S. Yu, F. Liu, Dimerization of rosin using Brønsted–Lewis acidic ionic liquid as catalyst, Catal. Commun. 9 (2008) 2030–2034. https://doi.org/10.1016/j.catcom.2008.03.045.

[38] W. Zhang, K. Xu, Q. Zhang, D. Liu, S. Wu, F. Verpoort, X.M. Song, Oxidative desulfurization of dibenzothiophene catalyzed by ionic liquid [BMIm]HSO_4, Ind. Eng. Chem. Res. (2010) 11760–11763. https://doi.org/10.1021/ie100957k.

[39] A.F. Ferreira, P.N. Simões, A.G.M. Ferreira, Quaternary phosphonium-based ionic liquids: thermal stability and heat capacity of the liquid phase, J. Chem. Thermodyn. 45 (2012) 16–27. https://doi.org/10.1016/j.jct.2011.08.019.

[40] D. Shang, X. Zhang, S. Zeng, K. Jiang, H. Gao, H. Dong, Q. Yang, S. Zhang, Protic ionic liquid [Bim][NTf_2] with strong hydrogen bond donating ability for highly efficient ammonia absorption, Green Chem. 19 (2017) 937–945. https://doi.org/10.1039/c6gc03026b.

[41] B.D. Cullity, S.R. Stock, Elements of X-Ray Diffraction, third ed., Prentice Hall, Upper Saddler River, 2001.

[42] F. Ragon, P. Horcajada, H. Chevreau, Y.K. Hwang, U.H. Lee, S.R. Miller, In situ energy-dispersive x-ray diffraction for the synthesis optimization and scale-up of the porous zirconium terephthalate UiO-66, Inorg. Chem. 53 (2014) 2491–2500. https://doi.org/10.1021/ic402514n.

[43] J.F. Olorunyomi, K.-Y. Chan, L. Gao, A.A. Voskanyan, C.-Y.V. Li, Direct synthesis of anion exchange polymer threaded in a metalorganic framework through in situ polymerization of an ionic liquid, Microporous Mesoporous Mater. 259 (2018) 255–263. https://doi.org/10.1016/j.micromeso.2017.08.054.

[44] J.F. Olorunyomi, K.-Y. Chan, L. Gao, A.A. Voskanyan, C.-Y.V. Li, Direct synthesis of anion exchange polymer threaded in a metal-organic framework through in situ polymerization of an ionic liquid, Microporous Mesoporous Mater. 259 (2018) 255–263. https://doi.org/10.1016/j.micromeso.2017.08.054.

[45] L. Ahmadian-Alam, H. Mahdavi, A novel polysulfone-based ternary nanocomposite membrane consisting of metal-organic framework and silica nanoparticles: as proton exchange membrane for polymer electrolyte fuel cells, Renew. Energy 126 (2018) 630–639. https://doi.org/10.1016/j.renene.2018.03.075.

[46] A.B. Yaroslavtsev, Y.P. Yampolskii, Hybrid membranes containing inorganic nanoparticles, Mendeleev Commun. 24 (2014) 319–326. https://doi.org/10.1016/j.mencom.2014.11.001.

[47] H. Furukawa, F. Gándara, Y.-B. Zhang, J. Jiang, W.L. Queen, M.R. Hudson, O. M. Yaghi, Water adsorption in porous metal−organic frameworks and related materials, J. Am. Chem. Soc. 136 (2014) 4369–4381. https://doi.org/10.1021/ja500330a.

[48] V.O. Mittal, H.R. Kunz, J.M. Fenton, Is H_2O_2 involved in the membrane degradation mechanism in PEMFC, Electrochem. Solid State Lett. 9 (2006) A299–A302. https://doi.org/10.1149/1.2192696.

[49] F.A.M. Loureiro, E.S. de Marins, G.D.C. dos Anjos, A.M. Rocco, Proton conductive membranes based on poly(styrene-*co*-allyl alcohol) semi-IPN, Polímeros 24 (2014) 49–56. https://doi.org/10.4322/polimeros.2014.070.

[50] K.D. Kreuer, On the development of proton conducting polymer membranes for hydrogen and methanol fuel cells, J. Membr. Sci. 185 (2001) 29–39. https://doi.org/10.1016/S0376-7388(00)00632-3.

[51] J.H. Chun, S.G. Kim, J.Y. Lee, D.H. Hyeon, B.-H. Chun, S.H. Kim, K.T. Park, Crosslinked sulfonated poly(arylene ether sulfone)/silica hybrid membranes for high temperature proton exchange membrane fuel cells, Renew. Energy 51 (2013) 22–28. https://doi.org/10.1016/j.renene.2012.09.005.